In Situ Quasi-elastic Neutron Scattering Study of the Hydration of Tricalcium Silicate

S. A. FitzGerald,* D. A. Neumann, and J. J. Rush

NIST Center for Neutron Research, National Institute of Standards and Technology, Gaithersburg, Maryland 20899

D. P. Bentz

Building Materials Division, National Institute of Standards and Technology, Gaithersburg, Maryland 20899

R. A. Livingston

Exploratory Research Team, Federal Highway Administration, McLean, Virginia 22101

Received August 13, 1997. Revised Manuscript Received October 30, 1997®

We report on the novel application of quasi-elastic neutron spectroscopy to study the reaction mechanism between tricalcium silicate and water. The in situ data taken at a series of fixed temperatures varying from 10 to 40 °C show that the amount of free water in the system remains relatively constant for an initial period, ranging from 1 h at 40 °C to 16 h at 10 °C. This is followed by an exponential decrease in the amount of free water that crosses over to a diffusion-limited behavior for later times. Fits to an Avrami type behavior allow us to determine an activation energy for the hydration process on the order of 30 kJ/mol.

Introduction

The reaction between tricalcium silicate (C_3S) and water is the principal factor in the setting and hardening of Portland cement. Given its importance, this reaction has been studied by numerous investigators in order to obtain a detailed understanding of the development of strength in concrete. However, the kinetics of the reaction and even the specific mechanisms are still not completely understood.

In this paper we report on the new application of quasi-elastic neutron scattering to study the hydration of tricalcium silicate. This technique provides a much more direct measure of the conversion of free water to bound water than previously used methods. It has the added advantage that measurements can be made in situ without disturbing the sample.

The overall hydration process which proceeds in several different reaction steps can be summarized as[1]

$$Ca_3SiO_5 + (3 + y - x)H_2O \rightarrow (CaO)_x(SiO_2)\cdot(H_2O)_y + (3 - x)Ca(OH)_2 \quad (1a)$$

which is written in cement notation as[2]

$$C_3S + (3 + y - x)H \rightarrow C_xSH_y + (3 - x)CH \quad (1b)$$

where x determines the Ca-to-Si ratio of the $C-S-H$ and y is the sum of hydroxyl ions and bound water molecules incorporated into the $C-S-H$ gel structure. Both x and y change over the course of the reaction and vary throughout the sample. $C-S-H$ is an amorphous gellike material which provides the cured paste's strength. However, the stoichiometry of the $C-S-H$ is still in doubt, and it is thought to occur in several different morphologies during hydration.[3] For a detailed study of this issue see the paper by Glasser et al.[4] The calcium hydroxide (CH) product is crystalline and hence yields to diffraction analysis.

The overall hydration of C_3S summarized in eq 1 consists of three separate chemical reactions. After mixing, the C_3S dissolves in an irreversible exothermic reaction[5]

$$Ca_3SiO_5(s) + 3H_2O \rightarrow 3Ca^{2+}(aq) + 4OH^-(aq) + H_2SiO_4^{2-}(aq) \quad (2)$$

Formation of the $C-S-H$ gel occurs through a secondary reaction in which

$$H_2SiO_4^{2-}(aq) + xCa^{2+}(aq) + (2x - 2)OH^-(aq) + (y - x)H_2O(l) \rightarrow (CaO)_x(SiO_2)\cdot(H_2O)_y \quad (3)$$

The Ca/Si ratio, x, of the gel product has been shown to vary both as a function of hydration time and

® Abstract published in *Advance ACS Abstracts*, December 15, 1997.

(1) Tarrida, M.; Madon, M.; Rolland, B. L.; Colombet, P. *Adv. Cem. Bas. Mater.* **1995**, *2*, 15.

(2) Cement-chemistry notation: C = CaO, S = SiO_2, H = H_2O.

(3) Diamond, S. *Cem. Concr. Res.* **1972**, *2*, 617.

(4) Glasser, F. P.; Lachowski, E. E.; Macphee, D. E. *J. Am. Ceram. Soc.* **1987**, *70*, 481.

(5) Tzschichholz, F.; Herrmann, H. J.; Zanni, H. *Phys. Rev. E* **1996**, *53*, 2629.

S0897-4756(97)00564-4
Published on Web 01/19/1998

temperature.[6-8] In general values range from 1 to 2 and in all cases the Ca/Si ratio is less than 3 and hence there is a buildup of Ca^{2+} ions in solution.[9] Once a critical concentration above the solubility limit has been reached, calcium hydroxide starts to precipitate out:

$$Ca^{2+}(aq) + 2OH^{-}(aq) \rightarrow [Ca(OH)_2](s) \quad (4)$$

These three reactions occurring throughout the curing process will be greatly affected by the ability of the different ions to penetrate surface coatings, migrate from one nucleation site to another, and diffuse into grains.

Due to its complex chemical and physical nature, it is difficult to arrive at a theoretically complete model of the kinetics of cement hydration. There are many divergent opinions regarding the details of the hydration mechanism which are well summarized in various review articles.[10,11] A generally accepted outline of the process is that immediately after mixing there is a brief burst of activity that is followed by a dormant period when the reaction rate decreases to a minimum. The dormant or induction period is thought to arise due to a surface layer of initial products coating the C_3S grains and inhibiting further reaction.[12] The rate stays at this minimum for a few hours (depending on temperature), after which the coatings apparently rupture. During the next period, the majority of the $C-S-H$ gellike material is formed through homogeneous nucleation and growth. When all of the available surface layers of the C_3S grains are coated with a sufficiently thick layer of $C-S-H$, the reaction becomes limited by the rate at which water can diffuse through the $C-S-H$ to reach the unreacted C_3S.

Quasi-elastic neutron scattering uses the principle that the elastic spectrum of neutrons scattered by a fixed (solid) material is distinctly different from that of neutrons scattered by a mobile (liquid) material. Such mobile scatterers produce a broadening in the elastic spectrum that increases with increasing mobility.[13] It is easy to separate out the fixed and mobile contributions to a spectrum and hence determine what fraction arises from solid material and what fraction from mobile, liquidlike material.

Due to hydrogen's extremely large incoherent scattering cross section, it tends to dominate neutron measurements in hydrogenous materials. More than 99% of the signal observed from our curing paste samples is due to scattering by hydrogen atoms. Since all of these atoms originated from the initial water mixed with the C_3S, our technique allows us to focus on the water and determine the fraction of molecules that are still liquidlike on a neutron time scale of $\sim 10^{-10}$ s. This fraction is referred to as the free water index (FWI).[14] It is expected to decrease throughout the hydration process as the free water is consumed either by being bound into the $C-S-H$ gellike structure or by chemically reacting to form calcium hydroxide.

The next section contains a brief description of the measurements. In the results section we demonstrate that the hydration process can be divided into three distinct stages: an initial induction period during which the FWI remains roughly constant, a growth period during which the FWI decreases exponentially with time and finally a diffusion-limited stage during which the FWI decreases more gradually with a simple power law dependence. In the analysis section, we model the data allowing us to extract temperature-dependent time constants for the growth period and diffusion constants for the final stage.

Experimental Procedure and Analysis Technique

The C_3S powder (Blaine of specific surface area 390 m^2/kg) obtained from Construction Technology Laboratories[15] is mixed with distilled water to produce a paste with a 0.4 water/C_3S ratio by mass. This is spread into a thin, 0.5 mm layer on an aluminum cell which is then sealed with an indium gasket. The sample is constrained to this thickness to mitigate the problem of multiple scattering. The cell is lined with Teflon to prevent the sample from reacting with the aluminum sample holder, which has been shown to delay the hydration process.[16] The sample is maintained at a constant temperature throughout the experiment. The results are averaged into 30 min slices with data being taken continuously for the first 48 h after mixing and thereafter at selected times for up to 60 days.

The quasi-elastic neutron scattering measurements are performed using the NIST Fermi chopper time-of-flight (TOF) spectrometer.[17] In this instrument an incident monochromatic beam of wavelength 4.8 Å first passes through a liquid nitrogen cooled beryllium filter and is then pulsed by a Fermi chopper. The length of the flight path after the sample is 2.29 m, which yields a resolution of 0.146 meV at the elastic scattering position. Results are averaged over a $|\bar{Q}|$ range from 1.9 to 2.4 $Å^{-1}$. $\bar{Q}$, the neutron scattering vector, is defined in terms of the change in neutron momentum upon scattering, $\bar{Q} = (\bar{P}_f - \bar{P}_i)/\hbar$.

In analyzing the data, we assume that the quasi-elastic energy-transfer spectrum can be divided into the sum of a component arising from bound hydrogen, $S_B(Q, \omega)$, and a component arising from mobile hydrogen (in the form of water), $S_F(Q, \omega)$. While the bound component can be simply represented by a delta function, the scattering of free water is complicated by the fact that both translational and rotational motions occur.[18] To achieve a sufficient time resolution to follow the hydration reaction, we must integrate the signal over an appreciable Q range, which further complicates the line shape. We therefore choose to follow a standard empirical approach in which the scattering from free water has been shown to be well represented by a simple Lorentzian function.[19] Despite the complicated motion of the water, this

(6) Skalny, J.; Odler, I. *J. Colloid Interface Sci.* **1972**, *40*, 199.
(7) Odler, I. *J. Appl. Chem. Biotechnol.* **1973**, *23*, 661.
(8) Bentur, A.; Berger, R. L.; Kung, J. H.; Milestone, N. B.; Young, J. F. *J. Am. Ceram. Soc.* **1979**, *62*, 362.
(9) Taylor, H. F. W. In *Cement Chemistry*; Academic Press Ltd.: London, 1990; pp 153-156.
(10) Taylor, H. F. W.; Barret, P.; Brown, P. W.; Double, D. D.; Frohnsdorff, G.; Johansen, V. *Mater. Constr.* **1985**, *17*, 457.
(11) Gartner, E. M.; Gaidis, J. M. In *Materials Science of Concrete*; J. P. Skalny, J.P., Ed.; American Ceramic Society: Westerville, OH, 1989; p 95.
(12) Odler, I.; Dorr, H. *Cem. Concr. Res.* **1979**, *9*, 277.
(13) Bée, M. *Quasielastic Neutron Scattering*; Adam Hilger: Bristol, 1988.
(14) Harris, D. H. C.; Windsor, C. G.; Lawrence, C. D. *Mag. Concr. Res.* **1974**, *26*, 65.
(15) Manufacturers are identified in order to provide complete identification of experimental conditions, and such identification is not intended as a recommendation or endorsement by the NIST.
(16) Livingston, R. A.; Neumann, D.; FitzGerald, S. A.; Rush, J. J. *SPIE* **1996**, *2867*, 148.
(17) Copley, J. R. D.; Udovic, T. J. *J. Res. Natl. Inst. Stand. and Technol.* **1993**, *98*, 71.
(18) Teixeira, J.; Bellissent-Funel, M. C.; Chen, S. H.; Dianoux, A. J. *Phys. Rev. A* **1985**, *31*, 1913.
(19) Blanckenhagen, P. *Ber. Bunsen-Ges. Phys. Chem.* **1972**, *76*, 891.

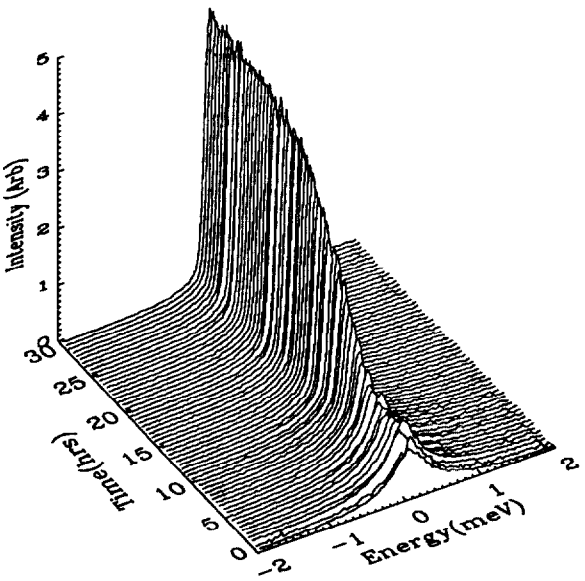

Figure 1. Time evolution of the quasi-elastic neutron spectra for C_3S cured at 20 °C. The water-to-C_3S ratio is 0.4 by mass and the elastic resolution is 0.146 meV.

simple approach is quite sufficient for our purposes of determining the fraction of free water.

In practice the finite resolution of the spectrometer must also be taken into account and thus the observed incoherent neutron scattering function is modeled by convoluting the Delta and Lorentzian peaks with a Gaussian function:

$$S_{inc}(Q,\omega) = \left\{A[\delta(\omega=0)] + B\left[\frac{\Gamma}{\pi(\Gamma^2+\omega^2)}\right]\right\} \otimes \left(\frac{1}{\sigma\sqrt{2\pi}} e^{-(1/2)(\omega/\sigma)^2}\right) \quad (5)$$

where A is the number density of bound hydrogen atoms, B is the number density of free hydrogen atoms (all of which are assumed to be in the form of water), Γ is the Lorentzian full width at half-maximum, and σ the Gaussian standard deviation is the measured resolution of the spectrometer.

The experimental data are fit to the expression in eq 5 with the free parameters of A, B, and Γ extracted. The agreement with our simple model is quite good considering the previously discussed complications. As a further check of our model, we examined the Q dependence of the scattering data over 4 h time-averaged slices. As expected for diffusive motions, Γ, the fwhm initially increases quadratically with Q before leveling off to a more constant value at higher Q.[13] In view of this, we perform our individual spectrum analysis over a $|\bar{Q}|$ range from 1.9 to 2.4 Å^{-1}, which is wide enough to produce sufficient statistics while keeping the spread in Γ and therefore deviations from a simple Lorentzian line shape to a minimum. We then define a free water index (FWI)[14] as FWI = $B/(A + B)$. Background corrections are achieved by measuring a dry cell containing just C_3S material. This ensures that the FWI is unity at the time of mixing.

Results

Figure 1 shows the data for the first 30 h for a sample cured at 20 °C. The 60 spectra shown are taken at 30 min intervals. At early times the spectra consist of a broad Lorentzian peak with almost no evidence of any sharp Gaussian component which would be indicative of bound water. The spectra remain relatively unchanged for the first 5 h before a sharp central Gaussian peak starts to emerge and then dominate at later times. The magnitude of the Gaussian component grows noticeably from one spectrum to the next until about 20 h has elapsed, after which the rate of change is much more gradual. The overall integrated intensity of the spectrum remains roughly constant throughout. The fact that the peak has become narrower makes it appear stronger at later times. The constant integrated intensity of the spectrum confirms that the sample is closed and that no water enters or leaves the system after it is sealed.

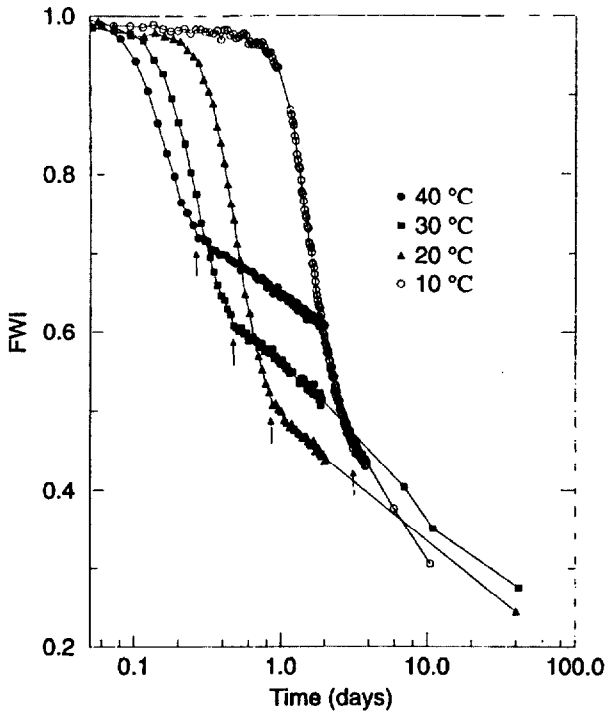

Figure 2. Free water index versus time for C_3S samples cured at 10, 20, 30, and 40 °C. The arrows indicate the sharp change in slope of the FWI at which point the reaction changes from a nucleation and growth to a diffusion-limited behavior.

It has been suggested that at high instrument resolution there exists a third spectral component resulting from highly constrained free water.[20] At the resolution of our spectrometer (0.146 meV) we see no evidence for this, and in all cases the behavior of the spectra follow very closely that of the two-component model outlined in eq 6. The main evidence we do observe for constrained behavior is that the width of the Lorentzian component becomes progressively narrower over the course of the reaction. This indicates that the mobility (translational or rotational) of the free water is in some way reduced at later curing times. This concept of constrained water will be the focus of a future study in which we use much higher instrument resolution to examine the precise Q dependence of the spectra.

Each spectrum shown in Figure 1 is fit to the sum of Gaussian convoluted delta and Lorentzian peaks whose intensity determine the FWI of the system at any given time. The hydration results for samples cured at 10, 20, 30, and 40 °C are shown as the FWI versus time on a log-linear plot in Figure 2. As expected, the curves start with the FWI very close to unity. In each case, the FWI initially decreases slowly until a time t_i when a sharp drop in the amount of free water is observed.

(20) Allen, A., private communication.

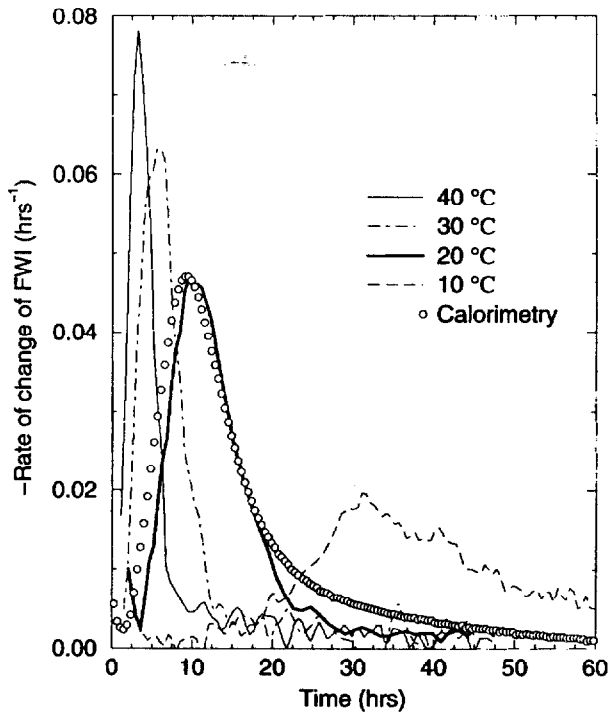

Figure 3. Rate of change of the free water index versus time. The calorimetry data was taken on a nominally identical sample that was kept at a fixed temperature of 20 °C.

Table 1. Parameters for the Three Stages of Hydration

					diffusion-limited		
	induction	nucleation and growth					$D^* \times 10^{15}$
T (°C)	t_i (h)	k (h^{-1})	A	n	t_d (h)	FWI_d	(m^2 h^{-1})
40	0.5	0.033	0.28	2.59	6.5	0.70	1.75
30	1.5	0.0174	0.39	2.27	11.0	0.61	2.42
20	3.5	0.0074	0.48	2.15	21.5	0.47	1.84
10	15.5	0.0019	0.52	1.88	80		

The duration of the initial dormant period depends on temperature varying from 0.5 h at 40 °C to 15.5 h at 10 °C. In all cases, only 1–3% of the free water is consumed during this initial period. This is in good agreement with the general findings from more traditional techniques.[10]

The second period begins with the sudden increase in the slope of the FWI and ends when the slope suddenly decreases. The termination point, t_d, indicated by the arrows in Figure 2 occurs progressively later with decreasing temperature. These times are included in Table 1. The final stage of the hydration process is diffusion-limited, during which time the FWI slope varies smoothly.

The kinetics of the hydration process are displayed in Figure 3 as the rate of change of the FWI (i.e., d(FWI)/dt) as a function of time. Also presented for comparison is an isothermal calorimetry curve showing the heat released at 20 °C for the same C_3S material. The two techniques show quite similar behavior with the peak in the heat release curve occurring slightly before the peak in the FWI rate. The peak of the FWI rate shifts to later times with decreasing temperature while its width increases. The peak shifts from 3 h at 40 °C, to 35 h at 10 °C. Consistent with a thermally activated process the change on going from 40 to 30 °C is much greater than that on going from 20 to 10 °C.

Rate Equations

There are many different models that attempt to explain the kinetics during each stage of hydration. The initial induction period is the least well understood, and since we have relatively few data points during this first stage we consider it only briefly. We define the end of the induction period to occur at the time when the differential of the FWI shown in Figure 3 rapidly increases from zero. Table 1 list the times, t_i, for each of the four temperatures, which follow very closely to a simple Arrhenius behavior, $t_i = t_0 \exp(-E_i/RT)$, with an activation energy, E_i, on the order of 36 kJ/mol. Although the times show a strong temperature dependence, the actual value of the FWI at the end of the induction period is relatively constant, lying between 0.97 and 0.99.

Following the induction period, C–S–H is formed through a process of nucleation and growth. We have determined through inelastic neutron spectroscopy that $Ca(OH)_2$ also starts to form at this time.[21] Our measurements indicate that during this period the ratio of the FWI signal arising from C–S–H growth to that occurring through $Ca(OH)_2$ formation is roughly 2:1. The rate of $Ca(OH)_2$ formation follows the same kinetic pattern as that of the decrease in the FWI which in turn mimics the rate of heat release. This suggests that during this stage the reaction rates are limited by the dissolution of C_3S and hence the same kinetic models that are traditionally used to predict the degree of hydration (α, defined as the fraction of C_3S that has dissolved)[9] can be applied to our FWI data. A standard approach is to model the nucleation and growth period with an Avrami behavior:[10,22–24]

$$\mathrm{FWI}(t) - \mathrm{FWI}(t_i) = 1 - A[1 - \exp(-k(t - t_i)^n)] \quad (6a)$$

$$\mathrm{d(FWI)/d}t|_{t \geq t_i} = -Akn(t - t_i)^{n-1} \exp(-k(t - t_i)^n) \quad (6b)$$

where t_i is defined as the time at which the induction period ends and nucleation and growth begins, A relates to the fraction of free water consumed, k is the rate constant and n depends on the dimensionality of the system and the type of growth.

Figure 4 shows fits to both the direct and differential forms of eq 6. The differential form is more sensitive to the fit parameters and has the added constraints that a peak occurs in d(FWI)/dt at time $t_m = ((n-1)/kn)^{1/n}$ and that the height of this peak is $\propto k^{1/n}$. The fit parameters listed in Table 1 show that the rate constant, k, progressively increases with temperature. To a much smaller degree n increases, and A decreases with increasing temperature. A nucleation and growth process should be temperature activated for which the rate constant follows an Arrhenius type relationship. The inset to Figure 4 confirms this behavior and determines the activation energy to be 30 kJ/mol.

(21) FitzGerald, S. A.; Neumann, D. A.; Rush, J. J.; Livingston, R. A., To be published.
(22) Brown, P. W.; Pommersheim, J.; Frohnsdorff, G. *Cem. Concr. Res.* **1985**, *15*, 35.
(23) Avrami, M. *J. Chem. Phys.* **1939**, *7*, 1103.
(24) Brown, P. W.; Pommersheim, J. M.; Frohnsdorff, G. In *Cements Research Progress*; Young, J. F., Ed.; The American Ceramic Society: Columbus, OH, 1983.

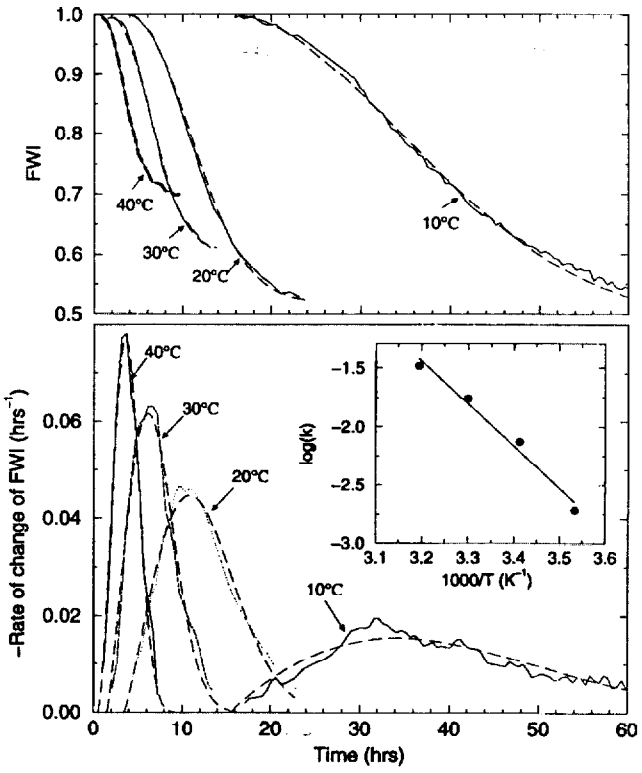

Figure 4. Fit of the nucleation and growth period data to an Avrami type behavior; solid line data, dashed line fit. (a) Shows the fit to the direct free water index. (b) Shows the fit to the differential of the free water index. The insert in (b) shows an Arrhenius plot of the rate constants, k, obtained from the Avrami fit.

This compares well with the results of free lime measurements,[25] 31.5 kJ/mol and of nonevaporable water data,[26] 33 kJ/mol.

The fits in Figure 4 indicate that the value of n is temperature dependent, changing from 1.9 to 2.6 on going from 10 to 40 °C. In physically interpreting this result we must remember that the FWI measurement probes both the formation of *CH* and *C–S–H*. However, an increase in n, which we assume to represent a general increase in the dimensionality of the growth phase (be it *C–S–H* or *CH*) is consistent with porosity measurements which show that the *C–S–H* is less dendritic and more closely packed at higher growth temperatures.[6–8] The only other temperature-dependent study which we know to have modeled their data to an Avrami behavior also finds n increasing from 2.12 at 20 °C to 2.27 at 40 °C.[27]

Diffusion-Limited Growth

After all the available surface area of the C_3S grains has reacted, the *C–S–H* can no longer be formed by nucleation and growth along the surface. The growth of the gel can continue only by growing inward into the C_3S grain.[25] Thus at this stage, the reaction becomes limited by the rate at which water can diffuse through the *C–S–H* surface layer to reach the unreacted C_3S. If we assume that the grains are spherical and that r is

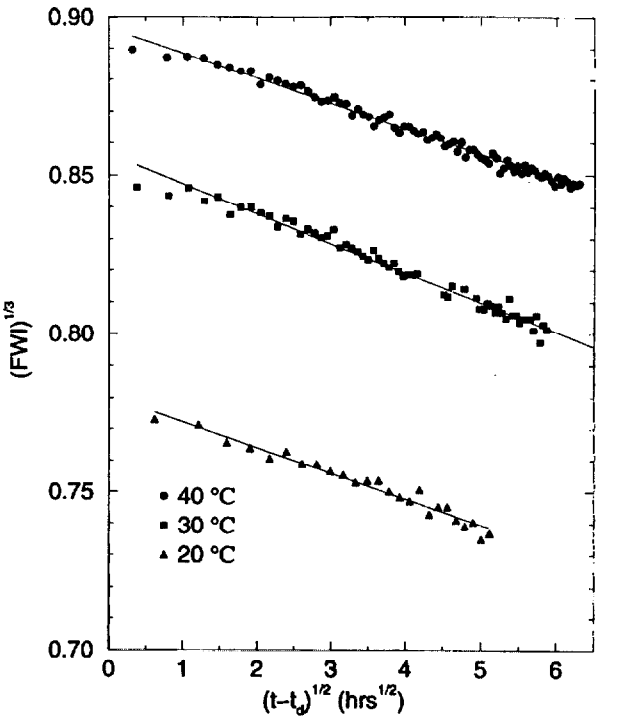

Figure 5. Free water index at later times fit to a diffusion-limited behavior. The values for t_d are listed in Table 1. Insufficient data were obtained at later times to establish the diffusion-limited behavior of the 10 °C sample.

the radius of the unreacted C_3S grain at time t, then[25]

$$dr/dt = D/(r - r_d) \tag{7a}$$

$$\rightarrow r_d - r = (2D)^{1/2}(t - t_d)^{1/2} \tag{7b}$$

where D is the appropriate diffusion constant and r_d is the radius of the C_3S at the time t_d when diffusion becomes the rate-limiting step. If we assume that the ratio of water molecules reacting with C_3S, expressed as $(3 + x - y)$ in eq 1, remains relatively constant throughout the diffusion-limited period then the FWI will scale with the volume fraction of unreacted C_3S, FWI $\propto (r/R)^3$, where R is the original radius of the C_3S grain. Expressing eq 7 in terms of the FWI yields

$$\mathrm{FWI}^{1/3} = (\mathrm{FWI}_d)^{1/3} - R^{-1}(2D^*)^{1/2}(t - t_d)^{1/2} \tag{8}$$

Equation 8 is written using D^*, an effective diffusion constant. D^* is related to D by the proportionality constant relating the FWI to the unreacted C_3S volume. For our initial water to C_3S ratio of 0.4 we expect that this constant is close to unity.

Figure 5 shows a plot of the data in terms of eq 8. The linear response for all three temperatures indicates that a diffusion-limited process dominates at later hydration times. The times, t_d indicating the onset of diffusion-limited behavior are listed in Table 1.

The effective diffusion constants, D^*, extracted from the fits in Figure 5 show relatively little change with temperature. Although this is consistent with a general trend that the latter stages of hydration are less sensitive to temperature,[7,8,10] one would still expect diffusion to be a thermally activated process which therefore should follow an Arrhenius behavior. One possible explanation for the observed temperature

(25) Fujii, K.; Kondo, W. *J. Am. Ceram. Soc.* **1974**, *57*, 492.
(26) Tenoutasse, N.; Donder, A. *Silicates Ind.* **1970**, *35*, 301.
(27) Double, D. D.; Hellawell, A.; Perry, S. J. *Proc. R. Soc. London A* **1978**, *359*, 435.

independence of D^* is that the activation energy for diffusion is much lower than that of the nucleation and growth process. Another consideration is that at higher temperatures the nucleation and growth process forms a denser $C-S-H$ layer around the C_3S grain.[6-8] The intrinsic increase in D^* due to a higher temperature is thus offset by having to diffuse through a more impervious medium. These two effects appear to combine to produce a net effect which is largely temperature insensitive.

This explanation for the behavior of the diffusion constant is also supported by the temperature dependence of FWI_d (the value of the FWI at the onset of diffusion-limited behavior). The results in Table 1 show that at 40 °C only 30% of the free water is consumed before time t_d, when diffusion-limited behavior sets in while at 20 °C, more than 50% is consumed. Since t_d defines the point at which the available C_3S surface area has been used up, this indicates that the water content of the $C-S-H$ formed up to this time is significantly lower at higher temperatures. This is consistent with the proposal that the high-temperature product forms a denser, more impenetrable coating around the C_3S grain.

Finally, it should be noted that in deriving eq 8 several factors have been ignored. Most important is the fact that the C_3S powder has a range of particle sizes. Particle size distribution analysis indicates that the grains have a median radius of 7.4 μm with 80% of them ranging between 2.5 and 20 μm. This broad distribution doubtless alters the kinetics of the diffusion process and leads to a large uncertainty in the absolute value of the diffusion constants listed in Table 1. However, the temperature dependence of the constants should be relatively unaffected by the distribution of grain sizes.

Summary

We have shown that quasi-elastic neutron scattering can be used to continuously monitor the amount of free water in hydrating cement. Data can be taken in situ without disturbing the sample at a time slice resolution of 30 min. Results show that hydration proceeds through an initial dormant period which becomes progressively longer with decreasing temperature. Following the dormant period the amount of free water decays with an Avrami time dependence. This behavior is controlled by a thermal activation energy of 30 kJ/mol. At longer times, the FWI decays more slowly in a process which is diffusion-limited and relatively temperature insensitive.

Acknowledgment. We would like to thank Edward Garboczi, Andrew Allen, and Nick Maliszewskyj (NIST) for numerous useful discussions.

CM970564A